MOSSBAUER SPECTROSCOPY OF Fe^{2+} BINDING TO APO AND HOLO MAMMALIAN FERRITIN

Richard B. Frankel
Department of Physics
California Polytechnic State University
San Luis Obispo, CA 93407

Gerald D. Watt
Department of Chemistry
University of Colorado
Boulder, CO 80309

and

Georgia C. Papaefthymiou
Francis Bitter National Magnet Laboratory
Massachusetts Institute of Technology
Cambridge, MA 02139

Abstract: The anaerobic binding of Fe^{2+} to apo and holo Mammalian ferritin has been studied in the pH range from 6.0 to 10.0. Mossbauer spectroscopy of samples in which the added Fe^{2+} is enriched in Fe-57 shows that the Fe^{2+} ions bind to the ferritin core and exchange electrons with Fe^{3+} ions in the core.

Introduction

Mammalian ferritin is a roughly spherical 24 subunit protein 130 A across containing a hollow interior 70 A across which can contain up to 4500 iron atoms in the form of an FeOOH mineral core. The function of the mammalian protein is to provide the cell with a readily mobilized, biologically compatible form of iron necessary for various metabolic purposes while simultaneously strongly binding iron and thereby protecting the cell from deleterious effects promoted by free cellular iron. The structure of the apo ferritin molecule has been reported (Treffrey and Harrison, 1984) at 2.8 A resolution and clearly shows the subunit arrangement and the hollow central interior where the iron mineral core is sequestered. The subunits are arranged in such a manner that channels leading from the exterior to the central cavity are formed along 3-fold (8 channels) and 4-fold (6 channels) symmetry axes. The 4-fold channels are essentially hydrophobic in nature, being lined with leucine amino acid residues, while the 3-fold channels are rendered hydrophyllic by carboxylate groups lining the channel interior . These crystallographic features have led to the hypotheses that Fe^{2+}, reductants/oxidants and chelators enter and leave the ferritin interior through these channel openings. Recent metal ion binding and binding competition studies (Treffrey and Harrison, 1984: Wardeska et al., 1986) have implicated the hydrophylic channels as binding sites for Fe^{2+}(as well as other metal ions that interact with ferritin) because 8 binding sites are observed, numerically equivalent to the 8 channels formed at the axis of 3- fold symmetry. The nature of the 4-fold channels remains undefined but a reasonable hypothesis is that these channels serve as reductant/oxidant entry ports or sites for redox reactions which alter the redox status of the ferritin core during iron release/iron deposition. Thus, a significant aspect of ferritin function is concerned with the role that these channels play in the regulation of cellular iron flux by the ferritin molecule.

The iron core of ferritin is another important feature of the ferritin structure that has received considerable study. X-ray and electron diffraction studies, electron microscopy as well as EXAFS measurments all have shown (Aisen and Listowsky, 1980; Theil, 1987) that the iron oxy-hydroxide core is a microcrystalline mineral, ferrihydrite. Mossbauer spectroscopy of the ferritin core has established that it is antiferromagnetically ordered at liquid helium temperatures (Oosterhuis nd Spartalian, 1976)) with superparamagnetic relaxation occuring as the material is warmed toward the Neel temperature.

The interaction of Fe^{2+} and other metal ions with apo ferritin has been studied recently using a variety of techniques and experimental approaches (Treffry & Harrison, 1984; Chasteen & Theil, 1982; Wardeska et al., 1985; Frankel et al. 1987) in an attempt to discern and study in some detail the role of Fe^{2+} in the events of core formation in mammalian ferritin. These studies have shown that: 1) the addition of Fe^{2+} to apo ferritin produces an initial complex which undergoes O_2-oxidation followed by rearrangement or migration of Fe(III) with polynuclear species ultimately forming within the ferritin core (Treffry & Harrison, 1984); 2) Fe^{2+} initially binds presumably at or near the hydrophilic channels with a stoichiometry of 8 Fe^{2+}/apo ferritin and that a mixed valent binuclear iron species forms when Fe^{2+} and Fe^{III}-core interact during early core formation (Wardeska et al., 1985; Wardeska et al., 1986); and 3) $^{57}Fe^{2+}$ binds strongly to both apo and holo ferritin forming ferritin bound Fe^{2+}, in the former case, and undergoing electron exchange with the core apparently forming surface bound $^{57}Fe^{3+}$ in the latter case (Frankel et al., 1985).

Other recent studies have examined the properties of Fe^{3+}-bound ferritin resulting from oxidation of Fe^{2+} initially added at low levels to mammalian apo ferritin. Mossbauer measurements (Bauminger et al., 1989) have demonstrated the presence of both solitary Fe^{3+} and oxygen bridged Fe(III) species which form early in the iron addition sequence but then give way to small Fe(III) clusters as more iron accumulates within the ferritin core. NMR relaxometry (Koenig et al. 1986) suggests that 6-8 unique Fe(III) sites presumably near the outside of each ferritin molecule are filled early during core formation and have large effects on solvent proton relaxation. The number of such sites remains constant with additional iron loading. EPR measurements (Rosenberg & Chasteen, 1982, see also below) support the early formation of 6-8 unique Fe3+ ions during core formation that remain constant as the core size increases. These results are all consistent with 6-8 Fe^{2+} initially binding at unique apo ferritin sites and undergoing subsequent conversion to Fe^{3+} upon oxidation. The number of unique Fe^{3+} ions remains constant with increased core filling suggesting a fundamental role for these species in core formation.

We have examined the quantitative binding of Fe^{2+} to both apo and holo mammalian ferritin and the subsequent conversion of these species to ferritin bound Fe^{3+} upon O_2-oxidation. Proton transfer during Fe^{2+} binding was observed in both apo and holo ferritin and appears to be an integral aspect of core development. These results relate directly to the early events of iron core formation and subsequent core development and are therefore very relevant to the mechanism of ferritin function in its iron storage role.

Materials and Methods

The horse spleen ferritin used in this study (2350 iron atoms per ferritin molecule) was obtained from Sigma and passed through G-25 columns to remove loosely bound metals. Total iron content was determined by the method of Lovenberg et al., 1963. Apo ferritin was prepared by dialysis against 0.1M thioglycollic/0.1M sodium acetate pH 4.25 until all iron was removed and then by dialysis against 0.025 M N-Tris(hydroxy-methyl) methyl-2-aminoethanesulfonic acid (TES), 0.1 M NaCl, pH 7.5 to remove the excess thioglycollic acid. The concentrated apo ferritin was noticeably yellow-brown in color but contained < 0.8 Fe/Apo ferritin molecule.

The equilibrium Fe^{2+} binding experiments were conducted under carefully controlled anaerobic conditions in an environmental chamber Fe^{2+} binding was determined by anaerobic G-25 Sephadex chromatography (Jacobs etal., Biochemistry, in press, 1989). Fe^{2+} bound to protein came off the column with the protein fraction whereas the unbound Fe^{2+} came off in a clearly separated band trailing behind the protein fraction. Protein and Fe^{2+} concentrations were determined by the Lowry and bipyridyl methods, respectively.

Fe^{2+} Binding to Apo Ferritin

Fig. 1a is a plot of Fe^{2+} bound to apo protein as a function of pH. These data were obtained by reacting apo ferritin for 30 minutes at the indicated pH with a 1-200 fold excess of Fe^{2+}; passing the sample through the G-25 Sephadex column and measuring the Fe^{2+} associated with the protein. Longer (>30 min.) or shorter (15 min.) incubation times did not change the Fe^{2+} binding values. The total amount of Fe^{2+} initially added was accounted for either in the protein band alone or in the protein band and in a separate Fe^{2+} band clearly separated from the protein, depending on whether limiting or excess Fe^{2+} was initially added. Control experiments on a calibrated column demonstrated that added Fe^{2+} emerged as a single band well behind the position of the solvent front indicating that aggregated Fe^{2+} species were absent and that Fe^{2+} found with ferritin was protein associated. Nearly constant values of 8.0 ± 0.5 Fe^{2+} associated with each apo ferritin molecule were obtained in the pH range 6-7.5. Above pH 7.5 the number of Fe^{2+} bound to apo ferritin dramatically increases with increasing pH until at pH 10.0 a value of 80 Fe^{2+}/apo ferritin is obtained. Some irreproducibility in the results was observed at pH >9, due perhaps to protein alterations at these higher pH values or $Fe(OH)_2$ formation upon Fe^{2+} addition, but those results presented in Fig. 1a were usually observed.

Fe^{2+}Binding in Holo Ferritin

Fig. 1b is a plot of Fe^{2+} bound to holo ferritin as a function of pH obtained by the G-25 Sephadex column method. As with apo ferritin, Fe^{2+} binding to holo ferritin is pH dependent but the degree of Fe^{2+} binding, at a given pH, is much greater with holo than with apo ferritin. The binding profile is also more complex with at least two distinct binding regions being clearly visible. Fe^{2+} binding below pH 6 was complicated because of protein precipitation as the isoelectric point (pH ~ 5.5) of holo ferritin was approached. Binding above pH 10 was erratic due to $Fe(OH)_2$ formation and possible alteration in the protein and core structures.

The strong pH dependence suggests proton release accompanies Fe^{2+} binding to holo ferrtitin, a result which has been verified experimentally (Jacobs et al., 1989).

Reversibility of Fe^{2+} binding to holo ferritin was only partially demonstrated. When holo ferritin (free of unbound Fe^{2+}) at pH 9-10 was adjusted to pH 6-7, free Fe^{2+} was formed but only 70-90% of that predicted from Fig. 1b. Increasing the incubation period at the lower pH tended to increase the amount of released Fe^{2+} but still incomplete (5-15% Fe^{2+} remaining) Fe^{2+} release was observed. Exposure of Fe^{2+} bound holo ferritin to O_2 resulted in conversion of the bound Fe^{2+} into Fe^{3+}, retained strongly by the protein.

Fig. 1 demonstrates a strong dependence of Fe^{2+} binding on pH in both apo and holo ferritin suggesting that protons are released or OH- ions are absorbed during the Fe^{2+} binding process. Direct pH measurements confirm the results of Fig. 1 by showing a pH decrease upon Fe^{2+} binding to either apo or holo mammalian ferritin. Rapid H^+ release occurs initially upon Fe^{2+} binding (within 1-2 min.) to both apo and holo ferritin but in the latter case this initial rapid H^+ release is followed by a much slower proton release "drift". This latter effect was much more noticeable at pH > 8.5 and occurred even in the absence of added Fe^{2+} indicating that the core itself is responsible for the "drift". Similar effects were noted by Silk and Breslow (1976) during acid/base titrations of deionized ferritin.

Mossbauer Spectroscopy

Iron-57 metal enriched to 95% (New England Nuclear-Dupont) was dissolved in 0.01M H_2SO_4 (50-70°C) under anaerobic conditions to produce $^{57}Fe^{2+}$ at concentrations of 0.01-0.1 M at pH 5-6.5. $^{57}Fe^{3+}$ was well below 1% of the total iron present. Excess $^{57}Fe^{2+}$ (50-100 fold excess for apo and 200-500 fold excess for holo) was added to 1.0 ml apo ferritin and holo ferritin samples (20-30 mg/ml) at pH 7.0 or 9.0, incubated anaerobically for 30 min and subsequently passed through 1 x 30 cm anaerobic G-25 Sephadex columns equilibrated at the corresponding pH to remove excess $^{57}Fe^{2+}$. An aliquot of each ferritin fraction was reacted with bipyridyl to determine the Fe^{2+}/ferritin ratio and to verify that the iron was present as $^{57}Fe^{2+}$.

The resulting apo ferritin samples containing bound $^{57}Fe^{2+}$ with no unbound Fe^{2+} present were used to prepare three samples (Table 1) for Mossbauer spectroscopy: the first, designated Apo(1), was $^{57}Fe^{2+}$ bound to apo ferritin at pH 7.0; the second, Apo(2), was $^{57}Fe^{2+}$ bound to apo ferritin at pH 9.0; and the third, Apo(3), was $^{57}Fe^{2+}$ bound to apo ferritin at pH 9.0 containing 1.0 mM $S_2O_4^{2-}$ to assure complete reduction.

The holo ferritin samples at pH 7.0 and 9.0 each containing bound $^{57}Fe^{2+}$ were divided into two separate portions. One portion was loaded into an air-tight plastic container and frozen. The other portion of each sample was exposed to air for one hour with gentle stirring to oxidize the added $^{57}Fe^{2+}$ to $^{57}Fe^{3+}$, then made anaerobic and incubated with excess non-isotopically enriched ferrous sulfate (2.2% iron 57) under argon for thirty minutes. After passage through an anaerobic Sephadex G-25 column, an aliquot was removed to verify that all added iron was in the Fe^{2+} state and the remainder was loaded into an air-tight plastic container and frozen. A total of four samples of ferrous bound holo ferritin were thus prepared for Mossbauer spectroscopy (Table I): Holo(1), 95% $^{57}Fe^{2+}$ bound holo ferritin at pH 7.0; Holo(2), natural Fe^{2+} (2.2% ^{57}Fe) bound holo ferritin following 95% $^{57}Fe^{2+}$ binding and oxidation at pH 7.0; Holo(3), 95% $^{57}Fe^{2+}$ bound holo ferritin at pH 9.0; Holo(4), natural Fe^{2+} bound holo ferritin following 95% $^{57}Fe^{2+}$ binding and oxidation at pH 9.0.

The Mossbauer spectra of Apo(1) and Apo(2) consisted primarily of a ferrous quadrupole doublet (isomer shift I.S.=1.26 mm/s, quadrupole splitting Q.S.=3.10 mm/s at 80K) and a residual ferric doublet (I.S.=0.47 mm/s, Q.S.=0.71 mm/s, approx. 6% of ferrous intensity). The residual ferric doublet was present even in samples where extreme measures were taken to assure anaerobic sample preparation. The spectrum of Apo(3) was a ferrous doublet with no residual ferric doublet. Thus, the ferric doublet in Apo(1) and Apo(2) appeared to arise from partial oxidation of the bound Fe^{2+} by the anaerobic apoferritin, in the absence of excess reductant.

Application of an 80 kOe external magnetic field to Apo(3) at 4.2K (data not shown) resulted in a broad, asymmetric spectrum similar to that reported for 10 ferrous ions bound to apoferritin by Yang et al. (1987). The spectrum reflected magnetic hyperfine interactions at the iron nuclei in addition to the applied magnetic field, indicating that the Fe^{2+} ions were bound in the high spin state and were not magnetically ordered at 4.2K.

The Mossbauer spectra of Holo(1) at 4.2, 20, 40, and 80K are shown in Figure 2. The spectra of Holo(2), Holo(3) and Holo(4) were similar. The spectra could be decomposed into subspectra corresponding to ferric and ferrous iron. The ferrous subspectrum consisted of a broadened quadrupole doublet at all temperatures. In Holo(4), the 80K ferrous subspectrum could be decomposed into two closely overlapping quadrupole doublets. The ferric subspectrum in all samples exhibited the superparamagnetic transition characteristic of fully oxidized ferritin (Oosterhuis and Spartalian, 1976) with a magnetic hyperfine split sextet at 4.2K and a quadrupole doublet at 80K. Between 4.2 and 80K, the ferric doublet and sextet were superposed with relative intensities that were temperature dependent. By definition (Frankel et al, 1987), the

average superparamagnetic blocking temperature $<T_B>$ is the temperature at which the doublet and sextet have equal intensities. The experimental values of $<T_B>$ were 29K, 27K, 34K and 30K for Holo(1), Holo(2), Holo(3) and Holo(4) respectively. In every Holo sample, $<T_B>$ was less than the average blocking temperature of fully oxidized ferritin ($<T_B>$=38-40K) and of ferritin electrochemically reduced by 40%, ($<T_B>$=51K) (Frankel et al, 1987).

It should be noted that the total absorption area of the ferric sextet at 4.2K is somewhat greater than the area of the ferric doublet at 80K. This appears to be a consistent feature of all the ferritin data we have accumulated. This difference in total absorption areas could be due in part to the temperature dependence of the recoilless fraction. However, data collected at higher temperature (See below) show that the ferric recoilless fraction is practically saturated below 80K. Another contribution to the difference in total area could arise from differential saturation effects in the two spectra, with the sextet lines less saturated than the doublet lines (Greenwood and Gibb, 1971). Data collected on samples of different thickness (not shown) show this effect does contribute, but apparently does not completely account for the difference. We are currently investigating the possibility that there are changes in the recoilless fraction associated with the superparamagnetic transition. In any case, even if the doublet and sextet absorption areas are normalized by the 80K doublet and 4.2K sextet absorption areas, respectively, the average blocking temperatures of the Fe^{2+}-bound Holo samples are still of the order of 5-10K less than fully oxidized ferritin.

In spectra obtained between 80 and 200K the ferrous absorption area decreased faster with increasing temperature than the ferric absorption area (Fig. 3). This is similar to partially reduced ferritin (Frankel et al, 1987). The ferric doublet of all the Holo samples had a temperature dependence of the absorption area similar to that of fully oxidized ferritin. The ferrous doublet had a temperature dependence of the absorption area similar to ferrous bound apo ferritin. The ferrous doublet of Holo(2) and Holo(4) decreased slightly faster with increasing temperature than that of Holo(1) and Holo(3).

The relative intensities of the ferric and ferrous doublets for the Holo samples are shown in Table 2. Assuming that no net oxidation of the bound ferrous ions occurred in the initial addition of Fe^{2+} to holo ferritin, the ferrous and ferric absorption areas at 80K would be proportional to the number of the respective ions with iron-57 nuclei in the sample if the recoilless fractions of Fe^{3+} and Fe^{2+} were equal at 80K. Considering the temperature dependence of Fe^{2+}in apo ferritin the Fe^{2+} recoilless fraction could be of the order of 10% lower than the Fe^{3+} recoilless fraction at 80K. The absorption areas corrected for this difference are included in Table 2. Even with this correction, the ferric doublet was more intense than expected in Holo(1) and Holo(3), whereas the ferrous doublet was more intense than expected in Holo(2) and Holo(4). Let us consider Holo(1) and Holo(3). If all the original 2565 Fe^{3+} ions per molecule remained Fe^{3+}, and all the added 95% $^{57}Fe^{2+}$ ions remained Fe^{2+}, we would expect on the average, Holo(1) to have 113 $^{57}Fe^{2+}$ and 50 $^{57}Fe^{3+}$, or ferrous and ferric relative absorption areas of 0.69 and 0.21, respectively. The corrected experimental values were 0.36 ferrous and 0.64 ferric for Holo(1). Holo(3) would be expected to have 309 $^{57}Fe^{2+}$ and 50 $^{57}Fe^{3+}$, or ferrous and ferric relative absorption areas of 0.86 and 0.14, respectively. The corrected experimental values were 0.59 ferrous and 0.41 ferric for Holo(3).

In Holo(2) and Holo(4), the original 95% iron-57 bound Fe^{2+} ions were oxidized, giving an average of 163 and 359 $^{57}Fe^{3+}$ per molecule, respectively. Subsequent addition of 2.2% iron-57 Fe^{2+} resulted in 2.5 $^{57}Fe^{2+}$ per molecule in Holo(2) and 7 $^{57}Fe^{2+}$ per molecule in Holo(4). Thus the expected relative absorption areas were 0.015 ferrous and 0.985 ferric in Holo(2); the corrected experimental values were 0.19 ferrous and 0.81 ferric. For Holo(4), the expected relative absorption areas were 0.02 ferrous and 0.98 ferric. The corrected experimental values for Holo(4) were 0.25 ferrous and 0.75 ferric.

Thus in Holo(1) and Holo(3), some of the added $^{57}Fe^{2+}$ was converted to Fe^{3+}, whereas in Holo(2) and Holo(4), some of the $^{57}Fe^{3+}$ bound in the core was converted to Fe^{2+} after addition of unenriched Fe^{2+}. A consistent interpretation of these results is that Fe^{2+}, when bound to holo ferritin under anaerobic conditions, enters the ferritin cavity, binds to the hydrous-ferric-oxide core and exchanges electrons with the ferric ions in the core. In Holo(1) and Holo(3) this process resulted in oxidation of the added $^{57}Fe^{2+}$ by Fe^{3+} ions in the core. In Holo(2) and Holo(4) this process resulted in reduction of $^{57}Fe^{3+}$ in the core by the added Fe^{2+}. The conversion of added $^{57}Fe^{2+}$ to $^{57}Fe^{3+}$ upon binding to the holo ferritin core was confirmed to be an "internal oxidation" as opposed to inadvertent oxidation (by O_2, for example) by reacting the Fe^{2+}-bound ferritin with bipyridyl and showing the original amount of added Fe^{2+} could be recovered. Inadvertent oxidation would have given a smaller Fe^{2+} recovery.

Entrance of Fe^{2+} into the cavity and binding to the core is also consistent with our previous observation that partial reduction by dithionite following Fe^{2+} binding preferentially reduces $^{57}Fe^{3+}$ to $^{57}Fe^{2+}$ (Frankel et al, 1987).

The lower average blocking temperatures of the Fe^{2+}-bound Holo samples compared to fully oxidized ferritin presumably reflect binding of the added $^{57}Fe^{2+}$ to the surface of the core particle. The $^{57}Fe^{3+}$ produced by oxygen or ferric ion oxidation would be sited predominantly near or on the surface of the core particle. In the theory of superparamagnetic relaxation as applied to ferritin (Oosterhuis and Spartalian, 1976), the electronic spins of all the ferric ions in the core particle relax at the same rate, which is an exponential function of particle volume/temperature. For a given particle volume, the blocking temperature is the temperature at which the spin relaxation rate equals the Larmor precession frequency of the iron-57 nucleus in the local magnetic hyperfine field. Possible explanations for the experimental decrease in the blocking temperatures of the surface ferric ions compared to the bulk include a decrease in the magnetic hyperfine field in the surface ferric ions. However, measurements of the hyperfine field distributions for the Holo samples show they are only marginally different than fully oxidized ferritin. It is also possible that the surface ferric ions form protoclusters that have smaller effective volumes than the bulk core particle with consequently lower blocking temperatures. Finally, it is also conceivable that the surface ferric ions relax at a faster rate than the bulk ions at the same temperature, especially those that are in contact with ferrous ions on the surface. In this regard it should be noted that in 40% reduced ferritin, the bulk blocking temperature increases compared to fully oxidized ferritin (Frankel et al, 1987). This latter effect may arise from the massive number of surface ferrous ions on the magnetic anisotropy of the core particle (Bell et al, 1984). Further investigation is required to elucidate the decrease of the blocking temperatures in the present case.

Discussion

As an iron storage protein, ferritin can accumulate large numbers of iron atoms (up to 4500 Fe/ferritin) in its interior in the form of an iron oxohydroxy mineral core. The mechanism by which apo ferritin initiates core formation, the number of sites involved and how further iron accumulation occurs once core formation is initiated has been the subject of a number of studies (Aisen & Listowsky, 1980; Theil, 1987; Crichton & Charlateau-Wauters, 1987). Recent spectroscopic studies (Chasteen & Thiel, 1982; Sayers et al. 1983; Treffry & Harrison, 1984; Wardeska et al., 1986) have shown that a finite number of metal ion binding sites (8-10) are present in the ferritin molecule where such metal ions as Cd^{2+}, Fe^{2+}, Fe^{3+}, Zn^{2+}, VO^{2+}, Mn^{2+}, and Tb^{3+} strongly and reversibly bind. For the most part, these studies have determined metal binding stoichiometries and relative affinities by measuring the competition for ferritin binding sites between two or more metal ions. An important outcome of these studies is that there appears to be different types of metal binding sites on apo ferritin, including more than one Fe(III) site (Treffry & Harrison, 1984; Chasteen & Theil, 1982). This latter conclusion is consistent with the hypothesis (Crichton et al., 1977; Chasteen & Theil, 1982; Treffry & Harrison, 1984) that

Fe^{2+} first binds to ferritin, undergoes oxidation to Fe^{3+} and then either undergoes transfer to or clustering in the ferritin interior.

The experiments that we report are relevant to the early events of ferritin iron core formation and clearly confirm and extend the previous binding studies discussed above. The results of Fig. 1 demonstrate, by direct methods, that Fe^{2+} has a strong affinity for and binds reversibly to apo ferritin with a stoichiometry of 8.0 ± 0.5 Fe^{2+}/apo ferritin in the pH range 6.0-7.5. Fe^{2+} and not Fe^{3+} is clearly the species being bound because of the strictly anaerobic conditions maintained during the experiments and because the analysis for bound iron measured both total iron as well as Fe^{2+} (as the bipyridyl complex) present in apo ferritin. The value of 8 Fe^{2+}/apo ferritin (0.33 Fe^{2+}/subunit) supports the view by Wardeska et al. (1986) that Fe^{2+} is bound in each of the eight hydrophilic channels located on 3-fold axes leading to the protein interior, although on the basis of the binding results alone the possibility can not be excluded that an 8 Fe^{2+} aggregate forms.

For the present, we interpret the results of Fig. 1a in terms of an eight site model below pH 7.5, but above this pH the results clearly show a dramatic increase in Fe^{2+} binding which we propose results from the formation of $Fe(OH)_2$ aggregates as the pH is raised above the hydrolysis threshold. As the pH increases, $Fe(OH)_2$ formation begins to occur at the original eight Fe^{2+} sites, increases with increasing pH and then begins to level off at 80 Fe^{2+} above pH 10. This leveling-off effect may be due to the saturation or filling of the region of ferritin near the initial Fe^{2+} binding sites because otherwise Fe^{2+} hydrolysis would not be expected to reach the limiting value shown in Fig. 1a. The process leading to Fe^{2+} binding at the higher pH values is reversible as demonstrated by adjusting the pH back to 7.0 and finding that all Fe^{2+} is released except for 8 Fe^{2+} bound to apo ferritin. This result is consistent with the neutralization of $Fe(OH)_2$ aggregates forming free Fe^{2+} which detaches from the unique Fe^{2+} binding site and enters the bulk solution.

Fig. 1b shows that Fe^{2+} binding to holo ferritin is dramatically different compared to that for apo ferritin, a result which is attributable to the presence of the core. Fig. 1b shows that below pH 6.0 Fe^{2+} binding approaches zero but rises rapidly above this value. Large numbers of Fe^{2+} are bound to holo ferritin under these higher pH conditions indicating that Fe^{2+} binding is probably occurring at multiple binding sites present on the mineral surface. The results in Fig. 1 b suggest that two types of binding sites are present, a low pH form functional below pH 8.5-9.0 and another above this value. The binding of Fe^{2+} to holo ferritin was not completely reversible with change of pH, with up to 15% of the original Fe^{2+} remaining bound to the holo ferritin. The internal redox reaction observed in the Mossbauer measurements (Table 2) and discussed later is probably the cause of this irreversibility.

An important aspect of metal ion binding to ferritin that has received only limited attention is the pH effects (Wardeska et al., 1985) accompanying metal ion interaction with apo ferritin. Fig.1 clearly reveals the differences in behavior of pH linked reactions occurring during the iron binding process in both apo and holo ferritin. For apo ferritin in the pH range 6-7.5, where 8 Fe^{2+} bind, there is a constant value of ~0.5 H^+ released for each Fe^{2+} bound. The source of this 0.5 proton release is not known but could arise from: 1) the ionization of protein side chains to which Fe^{2+} attaches or 2) the partial hydrolysis of Fe^{2+} after binding. Above pH 7.5, proton release per Fe^{2+} bound increases to a value near 1.5 at pH 9.0. At higher pH values, proton release measurements become quite difficult to quantitate but appear to approach a value of 2.0. This would be consistent with complete hydrolysis of the bound Fe^{2+} according to the following reaction,

$$Fe(H_2O)^{2+} = Fe(H_2O)_{n-2}\,(OH)_2 + 2H^+$$

a reaction perhaps consistent with the design and function of the ferritin molecule.

For holo ferritin, we interpret the results of Fig. 1b in terms of discrete but perhaps overlapping reaction steps involving Fe^{2+} binding to -OH groups present on the surface of the iron mineral core as represented in scheme I. Two equilibria are involved in this initial overall binding scheme:

Scheme I

1) ionization of the -OH groups forming $-O^-$ and 2) Fe^{2+} binding to ionized $-O^-$ groups. At low pH values, the surface oxygen atoms will be fully protonated (-OH) because protons out compete Fe^{2+} for the oxygen binding sites, thereby lowering the binding affinity of the core for Fe^{2+}. This prediction is consistent with the observations in Fig. 1b which shows that near zero Fe^{2+} binding occurs below pH 6. As the pH is increased from this low pH limit, Fe^{2+} binding increases because the equilibria of Scheme I becomes more favorable for Fe^{2+} binding at higher pH values. This prediction agrees with the results in Fig. 1b but is not quantitatively consistent with experimental results which show only $1H^+/Fe^{2+}$ released below pH 7.0. Scheme I shows the presence of two discrete -OH groups but this is no doubt an over simplification. The actual surface may have a complex distribution of many different -OH and $-O^-$ species which are likely to possess a range of ionization constants depending on their environment, and which, overall, produce on average ~ 1 H^+/Fe^{2+} bound. A notable result is that as the pH increases, an increase in H^+ release accompanies Fe^{2+} binding. This behavior is different from that predicted in Scheme I and suggests that another reaction becomes dominant in addition to or in place of that shown in scheme I. The Mossbauer results in Table 2 clearly reveal the presence of an internal redox reaction in which Fe^{2+} binds to the mineral surface and transfers an electron, apparently to the ferritin mineral core, and becomes surface bound Fe^{3+}. We propose that this newly formed, hydrated, surface-bound Fe^{3+} ion immediately begins to undergo a pH dependent hydrolysis, ultimately releasing three protons to the media. This overall process is depicted by the consecutive reactions in Scheme II. Such processes as outlined in Schemes I and II could be

$(H_2O)_n\ Fe^{2+} + \text{Core (Fe III)} = (H_2O)_n\ Fe^{2+} - \text{Core (Fe III)}$

$(H_2O)_n\ Fe^{2+} - \text{Core (Fe III)} = (H_2O)_n\ Fe^{3+} - \text{Core (Fe II)}$

$(H_2O)_n\ Fe^{3+} - \text{Core (Fe II)} = (H_2O)_{n-3}\ (OH)_3\ Fe^{3+} - \text{Core (Fe II)} + 3H^+$

Scheme II

responsible for the observed Fe^{2+} binding and H^+ release results shown in Fig. 1b and Table 2 at pH values 9.0 and below. Above this pH, long term pH drifts occur in the proton release measurements making interpretations less clear. These drifts arise from pH reactions occurring within the core which are independent of the Fe^{2+} binding process (Silk & Breslow, 1976) and may be due to pH induced alterations or aging of the ferritin core or the ferritin protein structure. It seems clear from our results and the interpretations that we suggest that the binding of Fe^{2+} followed by quite complex hydrolysis reactions are fundamental processes of the apo and holo ferritin molecules. As these processes are studied in more detail a clearer understanding of the mechanism of ferritin function is likely to emerge.

Acknowledgements

This work was supported by the U.S. National Science Foundation Biophysics Program and the U.S. Office of Naval Reaearch.

References

1. Aisen, P. & Listowsky, I. (1980) Ann. Rev. Biochem. 49, 375-393.
2. Bauminger, E. R., Harrison, P. M., Nowik, I. & Treffry, A. (1989) Biochemistry, in press.
3. Bell, S.H., Weir, M.P., Dickson, D.P.E., Gibson, J.F., Sharp, G.A., and Peters, T.J. (1984) Biochim. Biophys. acta 787, 227-236.
4. Chasteen, N. D. & Theil, E. C. (1982) J. Biol. Chem. 257, 7672-7677.
5. Colwick, S. P. & Womack, F. C. (1969) J. Biol. Chem. 244, 714-777.
6. Crichton, R. R. & Charloteaux-Wauters, M. (1987) Eur. J. Biochem. 164, 485-506.
7. Crichton, R. R., Collet-Cassart, D., Ponce-Ortiz, Y., Wauters, M., Roman, F. & Paques, E. (1977) in "Proteins of Iron Metabolism", eds. Brown, E. B., Aisen, P., Felding, J. & Crichton, R. R. Grune & Straton, N.Y. p. 13-22.
8. Frankel, R. B., Papaefthymiou, G. C. & Watt, G. D. (1987) Hyperfine Interactions, 33, 233-240.
9. Greenwood, N.N., and Gibb, T.C. (1971) "Mossbauer Spectroscopy", Chapman and Hall, London, pp. 659.
10. Koenig, S. H., Brown III, R. D., Gibson, J. F., Ward, R. J. & Peters, T. J. (1986) Magnetic Resonance in Medicine, 3, 755-767.
11. Lovenberg, W. M., Buchanan, B. B. & Rabinowitz, J. C. (1963) J. Biol. Chem. 238, 3899-3908.
12. Oosterhuis, W.T., and Spartalian, K. (1976) in "Applications of Mossbauer Spectroscopy", Vol. 1, ed. Cohen, R.L., Academic Press, New York, 141-170.
13. Rosenberg, P. L. & Chasteen, N. D. (1982) in "The Biochemistry and Physiology of Iron", eds. Saltman, P. & Hegenauer, J., Elsevier North Holland, Inc. p. 405-407.
14. Sayers, D. F., Theil, E. C. & Pennick, F. J. (1983) J. Biol. Chem. 258, 14076-14079.
15. Silk, S. T. & Breslow, E. (1976) J. Biol. Chem. 251, 6963-6973.
16. Theil, E. C. (1987) Annu. Rev. Biochem. 56, 289-315.
17. Treffry, A. & Harrison, P. (1984) J. Inorg. Biochem. 21, 9-20.
18. Wardeska, J. G., Viglione, B. J. & Chasteen, N. D. (1985) in "Proteins of Iron Storage and Transport", ed. Spik, G., Montrevie, J., Crichton, R. R., Mazurier, J. Elsevier Science, New York, N.Y. p. 85-88.
19. Wardeska, J. G., Viglione, B. & Chasteen, N. D. (1986) J. Biol. Chem. 261, 6677-6683.
20. Yang, C-y., Meagher, A., Huynh, B.H., Sayers, D.E. and Theil, E.C. (1987) Biochem. 26, 497-503.

Table 1. Mossbauer samples prepared by anaerobic binding of Fe^{2+} to apoferritin and to holoferritin containing an average number <n>=2565 Fe^{3+} per molecule.

Sample	pH	Original $^{57}Fe^{3+}$	Step 1 Added $^{57}Fe^{2+}$ [a]	Step 2 Added $^{57}Fe^{2+}$ [b]	Net $^{57}Fe^{2+}/Fe^{3+}$
Holo (1)	7.0	50	107 [c]	-	107/50
Holo (2)	7.0	50	107 [c]	3 [c]	3/157
Holo (3)	9.0	50	294 [d]	-	294/50
Holo (4)	9.0	50	294 [d]	-	7/344
Apo (1)	7.0	0	18	-	18/0
Apo (2)	9.0	0	61	-	61/0
Apo (3) [e]	9.0	0	61	-	61/0

(a) Fe^{2+} added as 95% iron-57.
(b) Fe^{2+} added as 2.2% iron-57 following oxidation of Fe^{2+} added in Step 1.
(c) Total Fe^{2+} bound = 133.
(d) Total Fe^{2+} Bound = 309.
(e) 1mM dithionite.

Table 2: Relative Ferric and Ferrous Iron-57 Mossbauer intensities in Holoferritin samples.

Sample		Experimental [a]	Corrected [b]	Theoretical [c]
Holo (1)	Fe 2+	0.34	0.36	0.68 (107)
	Fe 3+	0.66	0.64	0.32 (50)
Holo (2)	Fe 2+	0.17	0.19	0.02 (3)
	Fe 3	0.83	0.81	0.98 (157)
Holo (3)	Fe 2+	0.56	0.59	0.85 (294)
	Fe 3+	0.44	0.41	0.15 (50)
Holo (4)	Fe 2+	0.23	0.25	0.02 (7)
	Fe 3+	0.77	0.75	0.98 (344)

a) Experimental relative absorption areas at 80K.
b) Absorption areas corrected for temperature dependences of the recoilless fractions (see text).
c) Calculated relative concentrations of Fe^{2+} and Fe^{3+} assuming no electron exchange betweed added ferrous iron and ferric iron in the core particle. Numbers in parentheses are average iron-57 ions of each valence per molecule from Table 1.

Figure Captions

Figure 1. Fe^{2+} Binding to Apo and Holo Ferritin. a) The number of Fe^{2+} bound to two separate anaerobic apo ferritin samples, o, , in 0.025 M TES adjusted to the indicated pH values. Fe^{2+} binding in the presence of 0.5 mM $Na_2S_2O_4$, Δ. b) Fe^{2+} binding to holo ferritin (2086 Fe^{3+}/ferritin) under the same conditions as (a).

Figure 2. Mossbauer spectra of Holo(1) at 80, 40, 20 and 4.2 (top to bottom). The 80 K spectrum was fitted with a ferrous doublet (I.S.=1.34 mm/s, Q.S.=3.04 mm/s) and a ferric spectrum (I.S.=0.50 mm/s, Q.S.=0.71 mm/s). The relative intensities are given in Table 3. The ferric sextet spectrum corresponded to a magnetic hyperfine field distrubution with mode=497 kOe.

Figure 3. Normalized Mossbauer absorption areas plotted as a function of temperature for: (O) Apo (3) ferrous spectrum; (+) Holo (1) ferrous spectrum; (Δ) Holo (1) ferric spectrum.

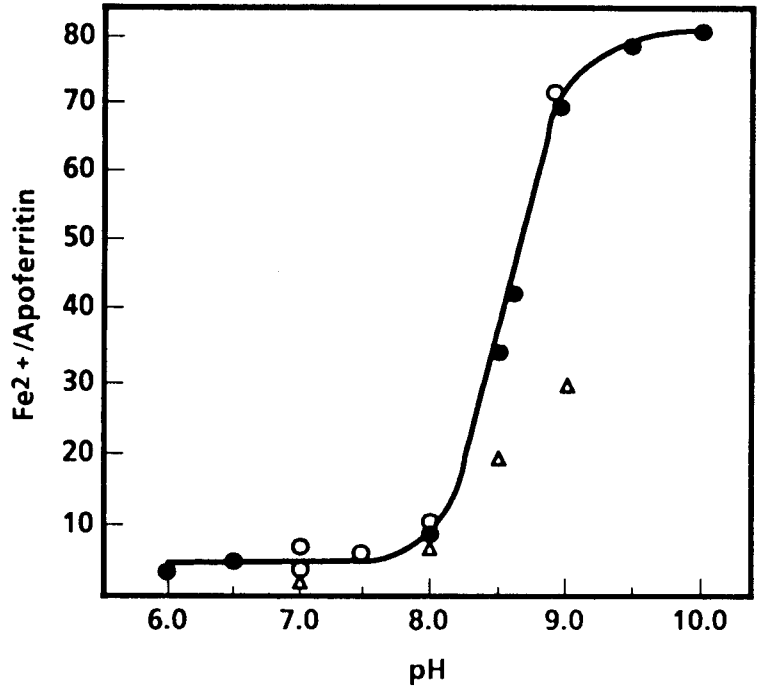

FIG. 1A

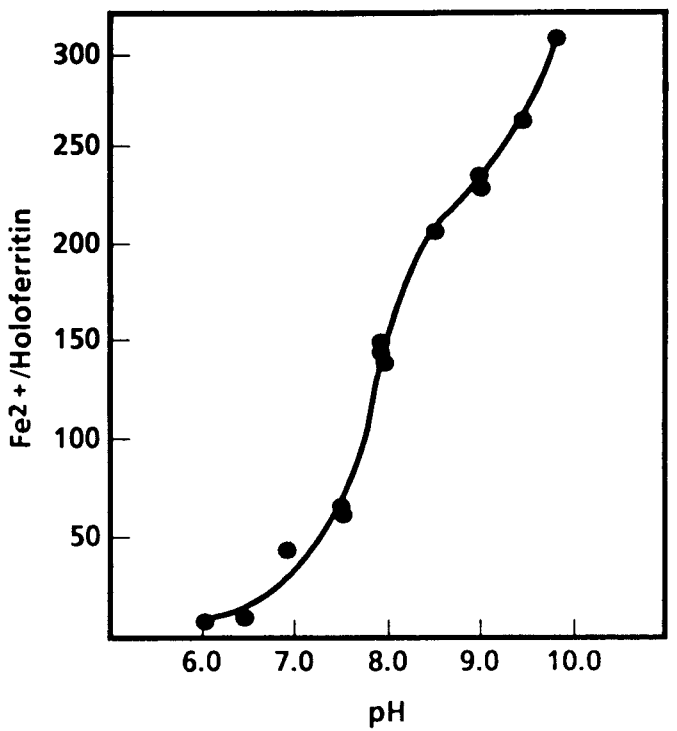
Fe2+/Holoferritin
300
250
200
150
100
50
6.0
7.0
8.0
9.0
10.0
pH

FIG. 1B

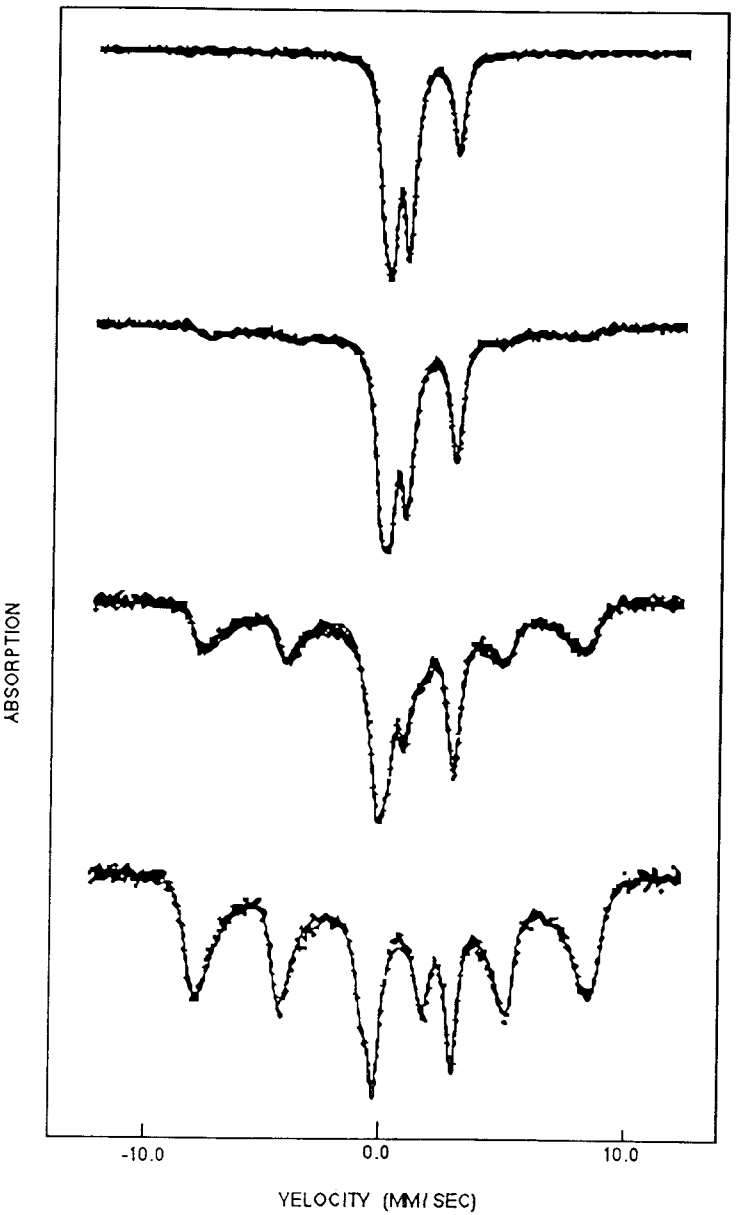
ABSORPTION
-10.0
0.0
10.0
VELOCITY (MM/SEC)

FIG. 2

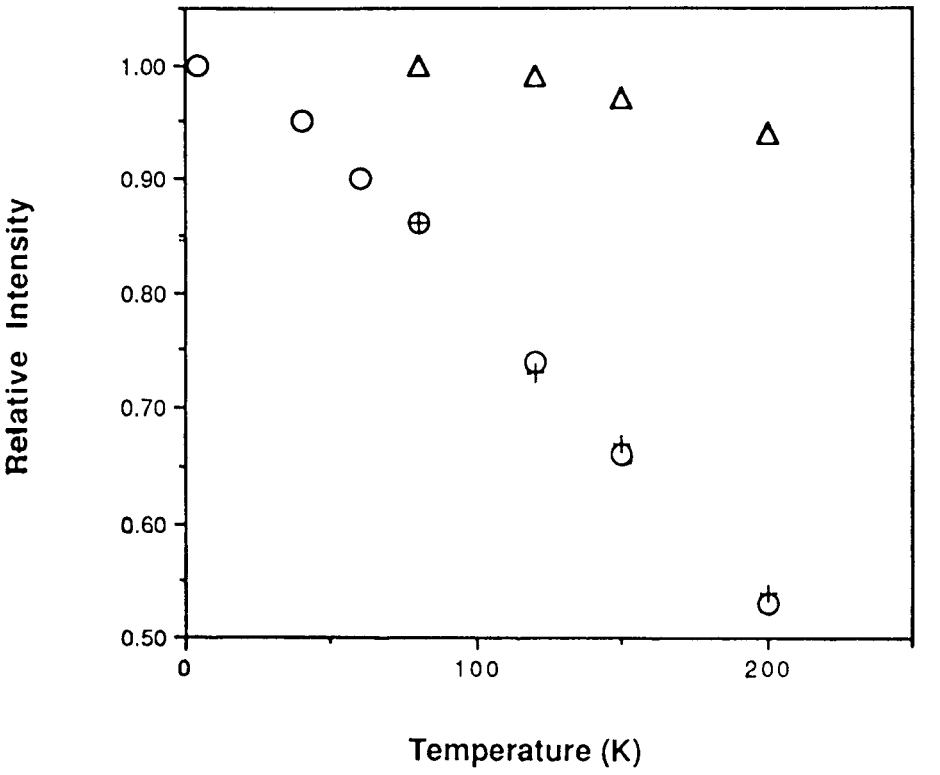
Relative Intensity
1.00
0.90
0.80
0.70
0.60
0.50
0
100
200
Temperature (K)

FIG. 3